Author response to Reviewer Comment 1: Zvi Steiner

Key:

- Review comment is in **bold**
- Author response is in normal text
- Changes made are in *italics*

We thank Dr. Zvi Steiner for their contribution to the review process of this paper. We have considered the reviewers comments carefully and incorporated their feedback in the below dialogue.

Baldry et al., report analyses of alkalinity and dissolved inorganic carbon along the main axis of the Red Sea and into some of the region's coastal ecosystem. These measurements are used to assess the magnitude of changes in total alkalinity and dissolved inorganic carbon in the various ecosystems of the Red Sea. The Red Sea has an exceptionally long stretch of tropical coastal habitats that are under increasing pressure globally. The unique oceanographic conditions of this region, e.g. relatively simple flow regime, high salinity and high temperatures turn the Red Sea into a very relevant site for studying how changes in different environmental variables affect coral reefs, mangroves and seagrass meadows. It is also a region that was historically very poorly represented in oceanographic studies.

This paper provides an important dataset which is an essential addition to the data currently available in the scientific literature. I think that the discussion of this data could be made substantially stronger if it will be better tied to previous publications and used to explain changes that were observed in the carbonate system of the Red Sea. As noted by the authors, there has be a large increase in the total alkalinity of the Red Sea surface waters in recent years (Steiner et al., 2018).

Previous publications on this topic were limited in their ability to assess if this change was only due to changes in coral calcification and ecology or there has been a shift in other ecosystems as well, and whether or not these correlate with each other. The authors chose to ignore half of their dataset and focus exclusively on the older samples but I think that comparisons between old and new trends of ecosystem specific rTA and rDIC could be valuable.

Together with comparison with past data regarding the change in DIC and total alkalinity of the central Red Sea axis, this can potentially provide a test for the various hypotheses previously suggested for the cause of the reduction in Red Sea calcification rates.

We thank the reviewer for the positive comments and the guidance provided. We focused our study in offshore Red Sea data published in the literature that is less than 10 years old, as well as new offshore data collected within the scope of the study to train our offshore model and calculate ecosystem specific rTA and rDIC. We noted a trend in TA and DIC in our offshore data compared to old cruises, which support the findings of Steiner et al. 2018. We are taking the reviewers comments on board and adding an extra subplot to Figure 4 to confirm the differences between old and new data with an independent dataset from 1982. This data will be made openly available via PANGAE upon acceptance of the manuscript.

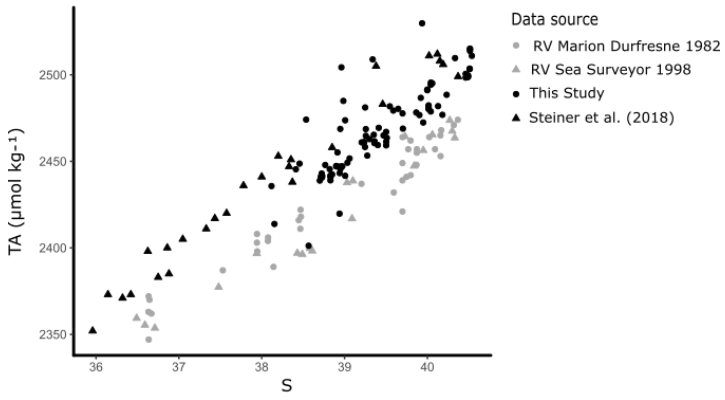

We also note that we did not include data reported in Steiner et al. (2018) in our published dataset. We have now added this data to our analysis, increasing the transition water dataset from 71 to 72 and the offshore dataset from 92 to 101. The inclusion has not changed the results or main findings of the paper substantially, and we will be happy to work this into our revised manuscript. A revised Section 3.1 and Table S2 is shown below to illustrate the minor changes the adding in the Steiner et al. (2018) data has to our model.

3.1 The Red Sea offshore end-member

The offshore carbonate system of the Red Sea was characterized along the south-north central axis. Offshore waters exhibited significant and strong (high r^2) linear increases in S, TA and DIC along the central south-north axis of the Red Sea as indicated by respective regression analysis with D (Figure 3, Table S3). TA and DIC were normalized to a salinity of 35 (nTA and nDIC), and both exhibited significant and weak (low r^2) linear decreases along the central south-north axis of the Red Sea (Figure 4). However, winter nDIC values appear to deviate from this linear relationship. The nTA and nDIC co-varied along this axis in an average ratio of 0.87 (SE= 0.07, r^2 = 0.60, F = 147.7, p<0.001) nTA to 1 nDIC (Figure 4c). A significant and weak (low r^2) linear decrease was found for T against D, that displayed clear seasonal dependencies between summer and winter/spring temperatures (Figure 3). A significant and weak (low r^2) increase in pH, a significant and weak (low r^2) decrease in pCO_2, and no significant linear relationship in Ω_A, against D were also observed.

In defining the offshore end-member for implementation in the single-end-member mixing model, offshore observations not representative of the expected linear relationships in the surface offshore Red Sea were removed. These were identified as eleven outlying offshore observations exhibiting a Cook's distance greater than five times the mean in at least one of the three linear models of D, against S, TA and DIC (Figure 1; Cook and Weisberg, 1997). Linear models were then re-fit with the remaining offshore observations (n = 104) to yield Equations 3-5, to be substituted into Equations 1-2 to complete the single-end-member mixing model (Figure 3).

Equation 3: $S_O = 0.00157*D + 37.47$

Equation 4: $TA_O = 0.0510*D + 2407$

Equation 5: $DIC_O = 0.0437*D + 2029$

*To approximate the error of the single-end-member mixing model, 99% prediction intervals (99% P.I. = mean ± 2.576*sd) were calculated by applying the single-end-member mixing model to offshore observations to yield rTA, rDIC, $rpCO_2$, rpH and $r\Omega_{Ar}$ (Table S2). These 99% P.I represent a cumulative error due to the natural variations of S_O, TA_O and DIC_O, along with the error propagation associated with the calculations of other carbon parameters. Two offshore observations used in defining the offshore end-member fell outside the 99% P.I., both exhibiting high TA, and one exhibiting high DIC.*

Table S2: *Defining statistics of the normal error for residual carbon variable estimates, as calculated from offshore observations*

	Residual mean	Residual standard deviation	Lower 99% P.I. bound^{+}	Upper 99% P.I. bound^{++}	% offshore observations outside the 99% P.I. (excluding/including outliers)
rTA (µmol/kg)	0	16.79	-43.25	43.25	1.1/5.9
rDIC (µmol/kg)	0	23.33	-60.09	60.09	2.2/5.9
rpH	-5×10^{-4}	2.69×10^{-2}	-6.97×10^{-2}	6.87×10^{-2}	4.3/6.9
$rpCO_2$ (µatm)	0.10	30.20	-77.69	77.90	4.3/7.9
$r\Omega_{Ar}$	0.0006	0.1879	-0.4833	0.4845	4.3/6.9

Whereas, the long-term trends observed in the Red Sea are not the focus of this study, we do believe that adding an element in the discussion using our new results to provide some insights onto the long-term changes noted by Steiner et al. (2018), will add value to the paper, as suggested by the reviewer. We have, therefore, added the following paragraph in the discussion section:

"The results reported here can offer explanation to the decadal changes in calcification rates in the Red Sea reported by Steiner et al. (2018), which are also supported by inspection of the data compiled

here (Figure 4a). Steiner et al. (2018), reported a 26 ± 16% decline in total $CaCO_3$ deposition rate along the basin between 1998 and 2018, concentrated in the southern Red Sea, suggesting that coral reefs in the southern Red Sea are under stress. Indeed, warming of the Red Sea, which has been faster than the global average (Chaidez et al. 2017), has been reported to reduce coral growth rates (Cantin et al. 2010), and massive bleaching of Red Sea corals south of 20ºN in the summer of 2015 (Hughes et al. 2018, Osman et al. 2018), and replacement by algal turf, may have reduced carbonate deposition rates in the southern Red Sea further. Our analysis suggests additional contributions to decline carbonate deposition in the Red Sea. In particular, mangrove habitats are characterized here as important sites of carbonate dissolution. Hence, the 13% increase in mangrove forests in the Red Sea over the past 30 years (Almahasheer et al. 2016), is expected to have resulted in increased rates of carbonate dissolution basin-wide."

Commented [CMD1]:

Commented [CMD2]:

Commented [CMD3]:

Commented [CMD4]:

Additional references.

Cantin, N. E., Cohen, A. L., Karnauskas, K. B., Tarrant, A. M. & McCorkle, D. C. Ocean warming slows coral growth in the central Red Sea. Science 329, 322–325 (2010).

Osman, E.O., Smith, D.J., Ziegler, M., Kürten, B., Conrad, C., El-Haddad, K.M., Voolstra, C.R. and Suggett, D.J., 2018. Thermal refugia against coral bleaching throughout the northern Red Sea. Global change biology, 24(2), pp.e474-e484.

Hughes, T. P. et al. Spatial and temporal patterns of mass bleaching of corals in the Anthropocene. Science 359, 80–83 (2018).

Chaidez, V., Dreano, D., Agusti, S., Duarte, C.M. and Hoteit, I., 2017. Decadal trends in Red Sea maximum surface temperature. Scientific reports, 7(1), p.8144.

A few specific comments:

Please refrain from using the shortcuts OCP and D. They are not intuitive and had me going back to check their meaning several times.

Noted. We will remove the acronym OCP. However, we need to retain the acronym D, as it is a key model parameter that we define in the methods and in Figure 2. We have edited the methodology to make what D more obvious to the reader by defining it first in the single end-member model.

OCP replaced with other carbon parameter. First paragraph of 2.4 now reads:

"A single-end-member mixing model was used to model conservative TA (cTA) and conservative DIC (cDIC) for coastal observations. First, the perpendicular distance of a point along the central axis of the Red Sea in km (D) was calculated for each observation. This was done using the "alongTrackDistance" function (default settings) in the R package "geosphere" (Hijmans, 2017) with the reference point 12.7737°N 43.2618°E to represent D = 0 and the reference point 28.2827°N 34.0694°E to define position of the central south-north axis. The single-end-member model was then implemented by 1) describing the linear variations of S, TA and DIC with D, so that predictions of offshore S (S_O), offshore TA (TA_O) and offshore DIC (DIC_O) can be made from D corresponding to coastal observations, and then 2) calculating cTA and cDIC for coastal observations according to Equations 1-2, which predict the simple dilution and concentration (SDC) effects of coastal evaporation (Figure 2)."

Caption edited from "……. O_i represents a location in the offshore end-member lying along the central axis at distance D_i,….." to "……. O_i represents a location in the offshore end-member lying along flow axis 1 (the central axis) at distance D_i,….."

Fig. 3: please indicate in the figure legend if these are surface waters only.

Noted.

"Observations of S, T and carbon variables in the offshore end-member (left)" changed to "Observations of S, T and carbon variables in the surface offshore end-member (left)"

Fig. 6: I don't understand from the legend what A, B, C, AB etc. stand for. It needs to be explained in the paper, not in the appendix.

Noted.

Figure 7 caption changed from "Grouping letters indicate the results of post-hoc bootstrapped t-tests, summarized from statistics presented in Table S5. If tests showed significant similarities at the 0.05 significance level with another habitat across a variable they were assigned the same letter." to "Grouping letters (A-D) assigned above boxplots indicate the results of post-hoc bootstrapped t-tests, summarized from statistics presented in Table S5. If tests showed significant similarities at the 0.05 significance level with another habitat across a variable they were assigned the same letter."

Fig. 7: From which year is the data presented here?

2016/2017.

Figure 7 x-label changed to month/year (below). Mm/dd is a mistake. Thank you!

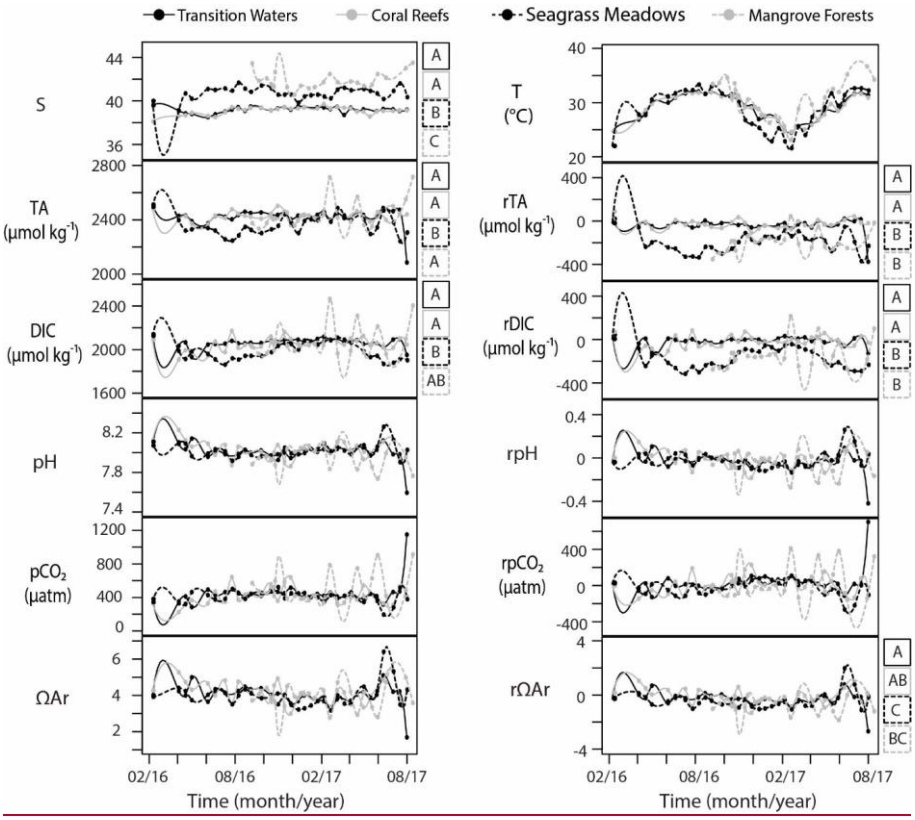
Transition Waters
Coral Reefs
Seagrass Meadows
Mangrove Forests
S
TA (µmol kg-1)
DIC (µmol kg-1)
pH
pCO2 (µatm)
ΩAr
T (°C)
rTA (µmol kg-1)
rDIC (µmol kg-1)
rpH
rpCO2 (µatm)
rΩAr
02/16
08/16
02/17
08/17
Time (month/year)